

First identification of *PODXL* nonsense mutations in autosomal dominant focal segmental glomerulosclerosis

Fu-Jun Lin^{1*}, Lei Yao^{2*}, Xue-Qing Hu^{3*}, Fan Bian¹, Gang Ji¹, Geng-Ru Jiang¹, Daniel P. Gale^{4#}, Hong-Qi Ren^{3#}

¹ Renal Division, Department of Internal Medicine, Xin Hua Hospital Affiliated to Shanghai Jiao Tong University School of Medicine, Shanghai 200092, China

² Sichuan Provincial Academician (Expert) Workstation, The Affiliated Hospital of Southwest Medical University, Luzhou, 646000, Sichuan Province, China

³ Department of Nephrology, 97th Hospital of PLA, Xuzhou 221004, Jiangsu Province, China

⁴ UCL Centre for Nephrology, Royal Free Hospital, London NW3 2PF, United Kingdom

*The first 3 authors contributed equally to this work.

#Correspondence and offprint requested to: Hong-Qi Ren; Email: sznk2005@163.com;

Daniel P. Gale; Email: d.gale@ucl.ac.uk

Abstract

Recently, a novel heterozygous missense mutation c.T1421G (p. L474R) in the *PODXL* gene encoding podocalyxin, was identified in an autosomal dominant focal segmental glomerulosclerosis (AD-FSGS) pedigree. However, this *PODXL* mutation appeared not to impair podocalyxin function and it is necessary to identify new *PODXL* mutations and determine their causative role for FSGS. In this study, we report the identification of a heterozygous nonsense *PODXL* mutations (Arg326X) in a Chinese pedigree featured by proteinuria and renal insufficiency with AD inheritance by whole exome sequencing (WES). Total mRNA and *PODXL* protein abundance were decreased in available peripheral blood cell samples of two affected patients undergoing hemodialysis, compared to those in healthy controls and hemodialysis controls without *PODXL* mutation. We identified another novel *PODXL* heterozygous nonsense mutation (c.C1133G; p.Ser378X) in a British-Indian pedigree of AD-FSGS by WES. In vitro study showed that, human embryonic kidney (HEK) 293T cells transfected with the pEGFP-*PODXL*-Arg326X or pEGFP-*PODXL*-Ser378X plasmid expressed significantly lower mRNA and *PODXL* protein compared to cells transfected with the wild-type plasmid. Blocking nonsense-mediated mRNA decay (NMD) significantly restored the amount of mutant mRNA and *PODXL* proteins, which indicated that the pathogenic effect of *PODXL* nonsense mutations is likely due to NMD, resulting in podocalyxin deficiency. Functional consequences caused by the *PODXL* nonsense mutations were inferred by

siRNA knockdown in cultured podocytes and podocalyxin downregulation by siRNA resulted in decreased RhoA and ezrin activities, cell migration and stress fiber formation. Our results provided new data implicating heterozygous *PODXL* nonsense mutations in the development of FSGS.

Key words: focal segmental glomerulosclerosis, podocyte, proteinuria, renal failure, genetic kidney disease

Abbreviations list

FSGS: focal segmental glomerulosclerosis

AD: autosomal dominant

WES: whole exome sequencing

PBMCs: peripheral blood mononuclear cells

PCR: polymerase chain reaction

GAPDH: glyceraldehyde-3-phosphate dehydrogenase

SDS-PAGE: SDS-polyacrylamide gel electrophoresis

siRNA: small interfering RNA

HRP: horseradish peroxidase

FP: foot processes

SD: slit diaphragm

hPSCs: human pluripotent stem cells

Introduction

Podocytes are terminally differentiated pericyte-like cells with a complex architecture that have an important role in the structure and function of the glomerular filtration barrier [1]. Primary podocytopathy, caused by podocyte injury or loss, can manifest with proteinuria, nephrotic syndrome and/or renal impairment in children and adults and is frequently associated with histological appearances of focal segmental glomerulosclerosis (FSGS) [2]. A minority of podocytopathy is due to genetic mutations, which affect proteins that are expressed in a variety of locations within a podocyte. Currently, mutations that cause podocyte structural and functional alterations have been found in more than 30 genes in human. These genes can mainly be divided into the following categories [3]: 1) podocyte slit diaphragm-associated molecules (*e.g.*, *NPHS1*, *NPHS2* and *CD2AP*), 2) actin-binding complexes within the foot process actin network (*e.g.*, *ACTN4*, *INF2*, *ANLN*, *ARHGAP24*), 3) actin regulation by RHO/RAC/CDC42 (*e.g.*, *ARHGAP24*, *ARHGDIA*, *KANK1/2*), 4) podocyte transcription factors (*e.g.*, *WT1*, *LMX1B* and *PAX2*), 5) mitochondrial function (*e.g.*, *COQ2*, *COQ6* and *PDSS2*), 6) cell/extracellular matrix (*e.g.*, *COL4A3/4/5*, *ITGB4* and *LAMB2*), 7) cell signaling (*e.g.*, *PLCE1* and *TRPC6*), 8) nuclear pore complex proteins (*e.g.*, *NUP93*, *NUP203* and *NUP107*), 9) cell membrane-associated proteins (*e.g.*, *PTPRO* and *EMP2*) and 10) lysosome (*e.g.*, *SCARB2*).

Inherited podocytopathy can present in infancy, childhood or adulthood [4].

Autosomal dominant (AD)-FSGS is characterized by later onset of disease and many patients exhibit proteinuria without nephrotic syndrome [5-7]. Recently, a novel heterozygous missense mutation c.T1421G (p.L474R) of the *PODXL* gene was identified in a Caucasian AD-FSGS pedigree by whole exome sequencing (WES) [8]. *PODXL* encodes podocalyxin, which plays an important role in the maintenance of structural integrity through the negative charge of the podocalyxin extracellular domain and by forming the podocalyxin/ezrin/actin complex required for the normal function of podocytes [9]. However, functional experiments showed that the p.L474R *PODXL* mutant did not alter *PODXL* protein stability, cell surface expression and subcellular localization, as well as binding to ezrin. Besides, this mutation of *PODXL* was not found 176 probands of AD-FSGS pedigrees. These results make the inference about a causal role of the L474R mutation in disease difficult. In the present study, we report heterozygous nonsense *PODXL* mutations in two unrelated pedigrees: c.C976T (p. Arg326X) in a Chinese pedigree that was associated with proteinuria and renal insufficiency, and c.C1133G (p. Ser378X) in an British-Indian AD-FSGS pedigree. We also provide evidence with in vitro study showing that the heterozygous nonsense *PODXL* mutations may be causative in AD-FSGS.

Methods

Subjects

Patients from the two pedigrees were enrolled in this study to investigate the causative genes of the glomerular disease. This study was approved by the Ethical Committee of Xin Hua Hospital affiliated to Shanghai Jiao Tong University School of Medicine (ref XHEC-D-2014-002) and West London Research Committee (ref 06-Q0406), respectively. Blood and urine samples from all subjects were collected with informed and written consent (including consent to publish) in accordance with the Declaration of Helsinki.

Whole exome sequencing and Sanger sequencing validation

DNA was extracted from blood samples using QIAamp DNA midi kit (Qiagen). Whole exome captures were performed on the probands of the two pedigrees using SureSelect Human All Exon 50 Mb Kit (Agilent). Paired-end sequencing (76 bp) was performed using the Genome Analyzer IIx (Illumina). Reads were aligned to the reference genome (GRCh37) using Novoalign (Novocraft, 2010). Variants were called using The Genome Analysis Toolkit (GATK) and annotated with ANNOVAR. To identify candidate variants, we adopted a filtering process to focus on non-synonymous novel deleterious variants using a combination of filtering against SNP databases (dbSNP and the 1000 Genomes Project), in-house exome data and prioritized according to genes association with renal phenotypes such as renal impairment, proteinuria, microscopic hematuria and abnormal kidney development after searching publicly available databases including PubMed, the Online Mendelian

Inheritance in Man (OMIM) and the Human Gene Mutation Database (HGMD).

Mapping and coverage data are summarized in Supplemental Table S1. Candidate variants identified by WES were validated by Sanger sequencing using an ABI PRISM 3730xl Genetic Analyzer (Applied Biosystems). Co-segregation of candidate variants was tested in all family members whose DNA sample was available.

Plasmid construction

Full-length human PODXL cDNA was subcloned into the MSC site (HindIII & BamHI) of the green fluorescence pEGFP-C1 vector to produce a recombinant plasmid, pEGFP-PODXL. Mutant pEGFP-PODXL plasmids with the p.Arg326X or p.Ser378X mutation were constructed using the Quikchange site-directed mutagenesis kit (QuikChange II Mutagenesis Kit, Qiagen). The primer sequences used to introduce the mutations were 5'-TCAACTACCCACTGATACCCCAAACAC-3' for p.Arg326X, 5'-GAAATTGATCTGACTGATATGCCGAGC-3' for p.Ser378X. The resulting two mutant plasmids pEGFP-PODXL-Arg326X and pEGFP-PODXL-Ser378X were sequenced to verify the incorporation of the required base changes.

Cell culture and transfection

Human embryonic kidney (HEK) 293T cells were cultured in Dulbecco's Modified Eagle's Medium (DMEM) supplemented with 10% fetal bovine serum (FBS),

100U/ml penicillin and 100U/m streptomycin at 37°C and 5% CO₂. HEK 293T cells were transfected with the wild-type pEGFP-PODXL plasmid or mutant pEGFP-PODXL plasmids using Lipofectamine 2000 (Invitrogen). The expression of plasmids was examined by a fluorescence microscope 48 hours after transfection. To inhibit NMD, wild-type and mutant pEGFP-PODXL plasmids-transfected cells were treated with 20 µg/ml of cycloheximide for 8 hours, and total RNA were analyzed by qRT-PCR. HEK 293T cells were sequentially transfected with *UPFI* small interfering RNA (siRNA) (5'-GACTCTGGTAATGAGGATTTA -3') and wild-type pEGFP-PODXL or mutant pEGFP-PODXL plasmids using Lipofectamine 2000 (Invitrogen) for 48 hours, and total RNA and proteins were analyzed by qRT-PCR and Western blot analysis.

The conditionally immortalized mouse podocytes (MPC5) were cultured in RPMI 1640 with 10% FBS and supplemented with recombinant mouse interferon- γ at 33°C. After differentiating at 37°C for 10-14 days without interferon- γ , MPC5 podocytes were transfected with siRNA targeting *PODXL* (5'-CCACTACACACAAACCATT-3') along with a siRNA control (RIBOBIO Biotech.) using Lipofectamine RNAiMAX (Invitrogen). Cells were harvested for various experiments 48-72 hours after transfection.

RNA extraction and quantitative RT-PCR assays

Peripheral blood mononuclear cells (PBMCs) were isolated from the whole blood of two affected patients (II-2 and II-3) in the Chinese pedigree, 6 maintenance hemodialysis patients without *PODXL* mutation and 6 healthy controls without *PODXL* mutation. RNA isolations from PBMCs, HEK 293T cells and cultured MPC5 podocytes after transfection were performed using RNeasy Mini RNA Isolation Kit (Qiagen). Then, 1 µg of total RNA was reverse-transcribed in a volume of 20 µl using random and oligo dT primers under standard conditions using the PrimeScript RT Kit (TaKaRa). For qRT-PCR assay, we used SYBR Premix Ex Taq (TaKaRa) to assess the mRNA level of *PODXL* in PBMCs, HEK293 cells and cultured MPC5 podocytes. The comparative $\Delta\Delta CT$ method of relative quantification was used to calculate for differences in gene expression using the software for ABI Prism 7500 sequence detection system (Applied Biosystems). The mRNA levels were normalized to glyceraldehyde-3-phosphate dehydrogenase (GAPDH).

Western blot analysis

Cell lysates from PBMCs, HEK 293T cells and cultured podocytes were prepared in RIPA extraction buffer supplemented with protease inhibitor cocktail. 20µg to 60µg protein was separated by 7.5-12% SDS-polyacrylamide gel electrophoresis (SDS-PAGE) and transferred to 0.22 µm PVDF membrane. After 1 h of incubation at room temperature in 5% dry milk powder, the membrane was incubated with the primary antibody against GFP (Cell Signaling Technology, 1:2000), podocalyxin

(Proteintech 1:500 for detection of podocalyxin in PBMCs and in HEK 293T cells; Novus 1:1000 for detection of podocalyxin in podocytes), anti-phosphorylated Thr567 of ezrin (Cell Signaling Technology, 1:1000), ezrin (Abcam, 1:1000), UPF1 (AB clonal, 1: 1000) , β -actin (Cell Signaling Technology, 1:1000) or GAPDH (Cell Signaling Technology, 1:1000), followed by incubation with the appropriate secondary antibodies. After immunoblotting, an ECL Plus Western Blotting System (GE Health) was used for detection.

RhoA G-LISA Assay

For the measurement of RhoA activity, a luminescence-based RhoA activity assay (G-LISA; Cytoskeleton) was used following the manufacturer's protocol. Briefly, cell lysates were prepared from cultured podocytes in which podocalyxin was knocked down and from control podocytes. The lysates were added to a Rho G-LISA plate coated with Rho-GTP-binding protein, followed by adding anti-RhoA primary antibody (diluted 1:250) and horseradish peroxidase (HRP)-labeled secondary antibody (1:250). After HRP detection reagent was then added, the luminescence signal of RhoA activity was detected using a multi-detection microplate reader (BioTek).

Immunofluorescence

Mouse podocytes growing on type I collagen-coated (Sigma-Aldrich) glass slides were pretreated with different conditions and then fixed in 4% paraformaldehyde for 10 minutes followed by being permeabilized in 0.2% Triton X-100 for 10 minutes. Rhodamine-labeled phalloidin (Beyotime) was used to stain F-actin in the podocytes, and the resulting images were examined by an inverted fluorescent microscope (Zeiss). The rhodamine-stained areas of the actin fibers were quantified using ImageJ software (NIH). The mean podocyte actin content per pixel and the total actin content per cell were calculated and expressed as AU.

Wound healing Assays

Mouse podocyte pretreated with different conditions were allowed to grow to confluence on type I collagen-coated (Sigma-Aldrich) culture dishes. Cell monolayers were washed and scratch wounds were applied using a 1000 μ l pipet tip. Podocytes were imaged using microscope at time 0 immediately after wound creation. Cells were then returned to growth restrictive conditions for 24 hours before final imaging of wound healing.

Transwell migration assay

Transwell cell culture inserts (Corning) were coated with type I collagen (Sigma-Aldrich), rinsed once with PBS, and placed in RPMI medium in the lower compartment. 1×10^4 mL⁻¹ control and PODXL knockdown podocytes were seeded in

the inserts and then allowed to migrate for 24 hours while being incubated at 37°C. Non-migratory cells were removed from the upper surface of the membrane and the migrated cells were fixed with 4% paraformaldehyde and stained with hematoxylin. The number of migrating cells was counted using phase contrast microscopy (Leica).

Statistical analysis

Continuous variables that were normally distributed were expressed as the mean \pm SD. Group differences were assessed by ANOVA with post-test correction (Bonferroni-Holm) or Student's t-test, as appropriate. A *P* value <0.05 was considered statistically significant.

Results

Case study of the Chinese pedigree with proteinuria and renal impairment

Figure 1A presents the pedigree of Chinese Han origin with proteinuria and renal insufficiency segregated as a dominant trait. The proband (III-1) was a 39-year-old male who first developed proteinuria (urinary albumin: creatinine ratio, ACR 100 mg/mmol) at the age of 25 with intact renal function, normal serum albumin level and normal blood pressure. He was found to have a declined renal function and then underwent renal biopsy at the age of 39. He received treatment with benazepril but his proteinuria persisted. Renal ultrasound examination revealed reduced renal cortical thickness. Serum creatinine (Scr) was 350 $\mu\text{mol/l}$. Two family members of III-1 (II-2

and II-3) had also developed proteinuria at the age of their 20s and 30s but received no treatment. Both of them progressed to end-stage renal disease at the age of 55 (II-3) and 72 (II-2), respectively. The III-2 (II-3's son) was 33 years old and had mild proteinuria (urinary ACR of 30-50 mg/mmol) and intact renal function at the time when he was recruited in this study. The II-2 and III-1 had mild microscopic haematuria. III-2 declined a renal biopsy. A summary of the renal phenotypes of the affected patients in the pedigree is presented in Table 1.

WES was performed on III-1 and no abnormality in the genes known to be associated with FSGS was identified except a *PODXL* heterozygous nonsense variant of c.C976T (p. Arg326X) in exon 4. The *PODXL* variant (rs367825197) is extremely rare. It is not found in the 1,000 genomes database and has an allele frequency of only 0.0001 in the NHLBI Exome Sequencing Project. Sanger sequencing (Figure 1B) confirmed this *PODXL* variant and its co-segregation with disease.

Because the patients' kidney tissues were unavailable, we examined *PODXL* mRNA and protein expression levels in PBMCs isolated from available peripheral blood samples of the two affected patients (II-2 and II-3) currently undergoing maintenance hemodialysis, as podocalyxin were reported to be expressed on haematopoietic cells in PBMCs [10]. Using CD34⁺CD45⁻ as the marker of hematopoietic cells [11], flow cytometry showed that the percentage of CD34⁺CD45⁻ cells were not significantly altered in PBMCs of II-2 and II-3 compared with those in the PBMCs of healthy controls (n=6) and maintenance hemodialysis patients (n=6) without *PODXL*

mutation (Supplementary Table 2, Supplementary Figure 1). Real-time PCR revealed a considerable reduction in *PODXL* mRNA expression in PBMCs of II-2 and II-3 compared with that of the healthy and hemodialysis controls (Figure 1C). Western blot analysis revealed decreased level of the *PODXL* core protein band (~55kDa) in II-2 and II-3 (Figure 1D) compared with that in the healthy and hemodialysis controls.

Case study of the autosomal dominant FSGS pedigree of Indian origin

After the identification of *PODXL* p. Arg326X heterozygous mutation in the Chinese pedigree, we reviewed WES data of FSGS pedigrees in the UCL Centre for Nephrology and identified a novel *PODXL* heterozygous nonsense mutation (c. C1133G; p. Ser378X) in exon 6 in the proband (I-1) of an AD-FSGS Indian pedigree (Figure 1E). Sanger sequencing (Figure 1F) confirmed this *PODXL* variant and its co-segregation with disease in the pedigree. Moreover, this variant was not present in healthy relatives or unrelated healthy controls. PBMC samples were unavailable from the Indian pedigree. A summary of the renal phenotypes of the affected patients in the Indian pedigree is presented in Table 1.

PODXL mutations (p.Arg326X and p.Ser378X) resulting in podocalyxin deficiency by triggering nonsense-mediated decay (NMD)

To further investigate the effects of *PODXL* nonsense mutations (p. Arg326X and p. Ser378X), plasmids expressing mutant pEGFP-*PODXL* plasmids were transfected

into HEK 293T cells at the same dose. 48 hours after transfection, cells transfected with pEGFP-PODXL-Arg326X or pEGFP-PODXL-Ser378X both revealed much weaker fluorescence signals than did those transfected with wild-type plasmid (Figure 2A). Under the same experimental settings, immunoblot analysis using antibodies against GFP showed that compared to those transfected with the wild-type plasmid expressing PODXL protein (~160 kDa), pEGFP-PODXL protein levels were greatly decreased in mutant-plasmid-transfected cell lysates (~75 kDa for Arg326X; ~100kDa for Ser378X) (Figure 2B). The mRNAs transcribed from the mutant plasmids were both significantly decreased (Figure 2C), and were rescued after the treatment with NMD inhibitor cycloheximide (Figure 2D). To confirm whether mutant mRNA is degraded via NMD, we used RNA-silencing to inhibit the core NMD factor UPF1 to suppress the NMD pathway and the result showed that in cells transfected with the mutant pEGFP-PODXL plasmids, downregulation of UPF1 by cotransfected with UPF1-siRNA significantly increased mutant pEGFP-PODXL mRNAs (Figure 2E) and protein levels (Figure 2F).

Podocalyxin downregulation leads to decreased activation of RhoA and ezrin, podocyte migration and F-actin stress fibers formation

Based on the observation that the two nonsense *PODXL* mutations are targeted by NMD and lead to podocalyxin deficiency, we performed *PODXL* knockdown to downregulate podocalyxin expression in mouse cultured podocytes in order to

investigate the molecular and cellular consequences of *PODXL* insufficiency.

Knockdown of podocalyxin by siRNA in the podocytes led to decreased activity of ezrin (Figure 3A and 3B) and RhoA (Figure 3C). In the wound-healing assay and transwell migration assay (Figure 4A-D), we found that podocytes showed decreased migration when podocalyxin was downregulated. Knockdown of podocalyxin also led to significantly reduced F-actin stress fibers in the podocytes (Figure 5A-B).

Discussion

In the present study, we report the identification of the heterozygous nonsense *PODXL* mutations (Arg326X) that may underlie the proteinuria and renal insufficiency clinically suggestive of AD-FSGS in the Chinese pedigree. In addition, we identified another novel heterozygous *PODXL* nonsense mutation (Ser378X) in an unrelated British-Indian pedigree of AD-FSGS, further supporting that nonsense mutations in the *PODXL* gene contribute to FSGS. We demonstrated that *PODXL* mRNA harboring the nonsense *PODXL* mutations identified in the two pedigrees was degraded through the NMD pathway, leading to reduced production of *PODXL* protein. The loss-of-function nature of the two nonsense mutations were supported by the observation that podocalyxin knockdown led to decreased activity of RhoA and ezrin, decreased migration and altered cytoskeletal structure of podocytes. Podocalyxin is a negatively charged, O-glycosylated and sialylated type I transmembrane protein [12] that is expressed primarily in podocytes and peritubular

capillaries but absent in tubules [13] in adult human kidney. Due to the essentiality of *PODXL* for the formation of the filtration barrier and the signals that mediate cytoskeletal organization of the foot processes, alterations in podocalyxin expression and function can induce podocyte injury and podocytopathies. Podocalyxin-deficient (*PODXL*^{-/-}) mice died within 24 h of birth due to anuric renal failure which was caused by the complete loss of foot processes (FP) and slit diaphragm (SD) [14]. During the preparation of this manuscript, a study came out and reported compound heterozygous *PODXL* mutations that led to complete loss of *PODXL* protein expression in a patient [15]. This patient presented with congenital nephrotic syndrome, omphalocele and microcoria, phenocopying the *PODXL*^{-/-} mice. In human pluripotent stem cells (hPSCs)-derived podocyte-like cells, knockout of podocalyxin caused defects in the organization of junctions and the spacing of adjacent podocyte-like cells [13].

Compared with the *PODXL*-null models, partial suppression of podocalyxin expression by morpholino antisense oligonucleotides resulted in poorly developed fine foot processes and hypoplasia of pronephric glomerulus in zebrafish morphants [16]. The *PODXL*^{+/-} mice with loss of one *PODXL* allele also displayed abnormal omphalocele during development but had no overt abnormality of FP and SD by electron microscopy [14]. Human diabetic nephropathy [17] and puromycin aminonucleoside-induced nephrotic mice [18] also exhibit reduced expression or sialylation of podocalyxin. In the study reporting the patient with congenital nephrotic

syndrome and compound heterozygous *PODXL* mutations, the *PODXL* construct with nonsense p.Trp341X mutation failed in expressing podocalyxin in contrast with wild-type *PODXL* [15], suggesting that nonsense *PODXL* mutations may induce NMD [19]. The above results are consistent with our in vitro study results that cells transfected with mutant pEGFP-*PODXL*-Arg326X or pEGFP-*PODXL*-Ser378X constructs resulted in considerably reduction in mutant pEGFP-*PODXL* mRNAs and *PODXL* protein levels via NMD in cell lysates. Previous study found that podocalyxin could be released to the extracellular space as intact protein or a soluble cleaved fragment of ectodomain [20-21]. In our in vitro study, full size *PODXL* protein (~160 kDa) was detected in the extracellular medium of HEK 293T cells transfected with wild type pEGFP-*PODXL* plasmid by Western blot analysis, whereas no *PODXL* protein was found in the extracellular medium of HEK 293T cells transfected with mutant pEGFP-*PODXL* plasmids (Supplementary Figure 2), probably due to deficient production of mutant *PODXL* protein via NMD.

Mechanistically, the basal activity of RhoA has been shown to be required for podocyte integrity [22], likely through its binding to ezrin to maintain the proper distribution of actin filaments and thus the architecture of the foot process [23]. We demonstrated the loss-of-function nature of *PODXL* nonsense mutations by knockdown of podocalyxin in cultured podocytes. We found that *PODXL* downregulation by siRNA led to significant decrease of RhoA activity, downregulation of ezrin phosphorylation, decrease of podocyte migration and

reduction of F-actin stress fibers in the podocytes. These effects of nonsense *PODXL* mutations are different from that of the missense *PODXL* mutation found previously in a Caucasian AD-FSGS pedigree in which podocalyxin expression was not altered but podocalyxin dimerization was facilitated [8].

Similar to the Caucasian AD-FSGS pedigree with heterozygous missense *PODXL* mutation, disease severities among the patients in the two pedigrees of this study were variable in terms of proteinuria and renal function. For example, the patient of III-2 in the Chinese pedigree had subtle clinical manifestation with only microproteinuria but normal renal function, whereas the renal function of his cousin (III-1) of similar age was already impaired with overt proteinuria. The intrafamilial clinical heterogeneity, e.g., proteinuria onset ranging from 10 to 54 years, might be due to other unknown modifying genes or environmental factors that affect the natural history of disease in different affected family members. Consistently, the mother of the patient with congenital nephrotic syndrome and compound heterozygous *PODXL* mutations (including the p. Try341X) [15] was apparently healthy although information on proteinuria was not provided.

In summary, we have identified pathogenic nonsense *PODXL* mutations in two unrelated pedigrees with clinical-suspected or biopsy-proven AD-FSGS and shown their adverse effects on cultured podocytes, which further implicated *PODXL* mutation in the development of FSGS.

Acknowledgements

The authors express their gratitude to patients and relatives who participate in this project.

Declarations of interest

None declared.

Funding information

FJL is funded by the National Natural Science foundation of China (grant no. 81500507), the Clinical Research Study Grant of Xin Hua Hospital Affiliated to Shanghai Jiao Tong University School of Medicine (grant no.17CSY03) and the Young Investigator Funding provided by Xin Hua Hospital affiliated to Shanghai Jiao Tong University School of Medicine (grant no. 2016-2018). DPG is funded by The Rosetrees and St Peters Trusts. LY is funded by the National Natural Science foundation of China (grant no. 81800301)

Author contribution

FJL, DPG, GRJ and HQR were responsible for the concept and design of the study.

FJL, DPG, FB and GJ were responsible for diagnosis, recruitment, clinical characterization and blood collection for all subjects studied. FJL and DPG analyzed

and interpreted the data. LY, XQH and HQR performed the functional experiments.

FJL, HQR and DPG wrote the manuscript.

References

1. Bryer J.S., Susztak K. (2018) Screening drugs for kidney disease: targeting the podocyte. *Cell Chem. Biol.* **25**, 126-127.
2. Bierzynska A., Soderquest K., Koziell A. (2015) Genes and podocytes - new insights into mechanisms of podocytopathy. *Front. Endocrinol.* **5**, 226.
3. Schlondorff J. (2015) How many Achilles' heels does a podocyte have? An update on podocyte biology. *Nephrol. Dial. Transplant.* **30**, 1091-1097.
4. Pollak M.R. (2014) Familial FSGS. *Adv. Chronic Kidney Dis.* **21**, 422-425.
5. Hao X., Xie J., Ma J., Wang Z., Zhou Q., Yang L., et al. (2013) Increased risk of treatment failure and end-stage renal disease in familial focal segmental glomerular sclerosis. *Contrib. Nephrol.* **181**, 101-108.
6. Brown E.J., Schlöndorff J.S., Becker D.J., Tsukaguchi H., Tonna S.J., Uscinski A.L., et al. (2010) Mutations in the formin gene INF2 cause focal segmental glomerulosclerosis. *Nat. Genet.* **42**, 72-76.
7. Barua M., Stellacci E., Stella L., Weins A., Genovese G., Muto V., et al. (2014) Mutations in PAX2 associate with adult-onset FSGS. *J. Am. Soc. Nephrol.* **25**, 1942-1953.
8. Barua M., Shieh E., Schlondorff J., Genovese G., Kaplan B.S., Pollak M.R. (2014)

Exome sequencing and in vitro studies identified podocalyxin as a candidate gene for focal and segmental glomerulosclerosis. *Kidney Int.* **85**, 124-133.

9. Schmieder S., Nagai M., Orlando R.A., Takeda T., Farquhar M.G. (2004) Podocalyxin activates RhoA and induces actin reorganization through NHERF1 and Ezrin in MDCK cells. *J. Am. Soc. Nephrol.* **15**, 2289-2298.
10. Kuhara M., Yoshino T., Shiokawa M., Okabe T., Mizoguchi S., Yabuhara A., et al. (2009) Magnetic separation of human podocalyxin-like protein 1 (hPCLP1)-positively cells from peripheral blood and umbilical cord blood using anti-hPCLP1 monoclonal antibody and protein A expressed on bacterial magnetic particles. *Cell Struct. Funct.* **34**, 23-30.
11. Kerosuo L., Juvonen E., Alitalo R., Gylling M., Kerjaschki D., Miettinen A. (2004) Podocalyxin in human haematopoietic cell. *Br. J. Haematol.* **124**, 809-818.
12. Nielsen J.S., McNagny K.M. (2009) The role of podocalyxin in health and disease. *J. Am. Soc. Nephrol.* **20**, 1669-1676.
13. Freedman B.S., Brooks C.R., Lam A.Q., Fu H., Morizane R., Agrawal V., et al. (2015) Modelling kidney disease with CRISPR-mutant kidney organoids derived from human pluripotent epiblast spheroids. *Nat. Commun.* **6**, 8715.
14. Doyonnas R., Kershaw D.B., Duhme C., Merkens H., Chelliah S., Graf T., et al. (2001) Anuria, omphalocele, and perinatal lethality in mice lacking the CD34-related protein podocalyxin. *J. Exp. Med.* **194**, 13-27.
15. Kang H.G., Lee M., Lee K.B., Hughes M., Kwon B.S., Lee S., et al. (2017) Loss

- of podocalyxin causes a novel syndromic type of congenital nephrotic syndrome.
Exp. Mol. Med. **49**, e414.
16. Ichimura K., Powell R., Nakamura T., Kurihara H., Sakai T., Obara T. (2013)
Podocalyxin regulates pronephric glomerular development in zebrafish. *Physiol.
Rep.* **1**, e00074.
17. Koop K., Eikmans M., Baelde H.J., Kawachi H., De Heer E., Paul L.C., et al.
(2003) Expression of podocyte-associated molecules in acquired human kidney
disease. *J. Am. Soc. Nephrol.* **14**, 2063-2071.
18. Kerjaschki D., Vernillo A.T., Farquhar M.G. (1985) Reduced sialylation of
podocalyxin-the major sialoprotein of the rat kidney glomerulus-in
aminomucleoside nephrosis. *Am. J. Pathol.* **118**, 343-349.
19. Fang Y., Bateman J.F., Mercer J.F., Lamandé S.R. (2013) Nonsense-mediated
mRNA decay of collagen-emerging complexity in RNA surveillance mechanisms.
J. Cell Sci. **126**, 2551-2560.
20. Fernández D., Larrucea S., Nowakowski A., Pericacho M., Parrilla R., Ayuso M.S.
(2011) Release of podocalyxin into the extracellular space. Role of
metalloproteinases. *Biochim. Biophys. Acta.* **1813**, 1504-1510.
21. Larrucea S., Butta N., Arias-Salgado E.G., Alonso-Martin S., Ayuso M.S., Parrilla
R. (2008) Expression of podocalyxin enhances the adherence, migration, and
intercellular communication of cells. *Exp. Cell. Res.* **314**, 2004-2015.
22. Wang L., Ellis M.J., Gomez J.A., Eisner W., Fennell W., Howell D.N., et al. (2012)

Mechanisms of the proteinuria induced by Rho GTPases. *Kidney Int.* **81**,
1075-1085.

23. Mouawad F., Tsui H., Takano T. (2013) Role of Rho-GTPases and their regulatory proteins in glomerular podocyte function. *Can. J. Physiol. Pharmacol.* **91**,
773-782.

Figure legends

Figure 1: Family pedigrees, sequencing results and decreased *PODXL* mRNA and protein levels in peripheral blood from the affected individuals with *PODXL*

p. Arg326X mutation. (A) The pedigree of Chinese Han origin with proteinuria and renal insufficiency segregated as a dominant trait. (B) Sanger sequencing of exon 4 of *PODXL* demonstrated a heterozygous C-to-T transition, which is predicted to result in a p.Arg326X mutation in the proband patient (III-1). (C) The bar graph showing the relative *PODXL* mRNA abundances as determined by quantitative PCR in peripheral blood mononuclear cells (PBMCs) of 6 unaffected healthy controls (NC: 1.0 ± 0.25), 6 maintenance hemodialysis (MHD: 1.09 ± 0.13) patients without nonsense *PODXL* mutations and 2 affected patients (II-2: 0.30 ± 0.02 ; II-3: 0.55 ± 0.03). *GAPDH* (glyceraldehyde-3-phosphate dehydrogenase) was used for normalization. The data represented the mean \pm SD of 3 independent experiments. *Significantly different from NC (ANOVA with post-test correction, $P < 0.05$), #Significantly different from MHD (ANOVA with post-test correction, $P < 0.05$). (D) Podocalyxin protein levels in PBMCs of 2 representative unaffected healthy controls (NC1 and NC2), 2 representative maintenance hemodialysis patients without nonsense *PODXL* mutations (MHD1 and MHD2) and 2 affected patients (II-2 and II-3) carrying the *PODXL* p.Arg326X mutation. Cell lysates from PBMCs were immunoblotted with anti-podocalyxin (upper panel) and with anti-GAPDH (lower panel) as a control for protein loading. (E) An Indian pedigree of biopsy proven AD-FSGS. (F) Sanger sequencing of exon 6 of *PODXL* of the proband patient (I-1) in the Indian pedigree

demonstrated a heterozygous C-to-G transition, which is predicted to result in a p.Ser378X mutation.

Figure 2: Mutant *PODXL* mRNA (p. Arg326X and p. Ser378X) are degraded via

nonsense-mediated decay (NMD). (A) HEK 293T cells transfected with wild-type

pEGFP-PODXL or mutant plasmids (pEGFP-PODXL-Arg326X;

pEGFP-PODXL-Ser378X) under the same conditions showed that the mutant

constructs exhibited lower fluorescence yield. Scale bar 100 μm (40x magnification).

(B) Immunoblot analysis using antibodies against GFP showed EGFP-fusion products

(~75 kDa for Arg326X; ~100 kDa for Ser378X) with considerably decreased protein

levels in mutant-construct transfected HEK 293T cells lysate than the EGFP-fusion

product (~160 kDa) in the cells transfected with the wild-type pEGFP-PODXL

plasmid. (C) pEGFP-PODXL mRNA expression in HEK 293T cells transfected with

mutant plasmids (pEGFP-PODXL-Arg326X or pEGFP-PODXL-Ser378X) were

significantly decreased compared with that in cells transfected with the wild-type

pEGFP-PODXL plasmid (WT: 1.0 ± 0.05 ; Arg326X: 0.11 ± 0.006 ; Ser378X:

0.11 ± 0.007). *Significantly different from the wild-type plasmid (ANOVA with

post-test correction, $P < 0.05$). (D) Treatment of cells with cycloheximide (CHX)

significantly increased pEGFP-PODXL mRNAs transcribed from the two mutant

plasmids (Arg326X without CHX: 0.05 ± 0.008 , Arg326X with CHX: 0.32 ± 0.02 ;

Ser378X without CHX: 0.07 ± 0.007 , Ser378X with CHX: 0.35 ± 0.01), but had no

effect on the pEGFP-PODXL mRNA level transcribed from the wild-type plasmid (WT without CHX: 1.0 ± 0.03 ; WT with CHX: 1.02 ± 0.05). * Significantly different from those without cycloheximide treatment (Student's t-test, $P<0.05$). (E) Inhibition of UPF1 in HEK 293T cells by RNA interference resulted in significantly increased mRNA of mutant pEGFP-PODXL harboring Arg326X or Ser378X mutation (Arg326X with si-ctrl: 0.1 ± 0.009 , Arg326X with si-UPF1: 0.27 ± 0.02 ; Ser378X with si-ctrl: 0.08 ± 0.02 , Ser378X with si-UPF1: 0.27 ± 0.02), whereas UPF1 siRNA had no effect on pEGFP-PODXL mRNA levels (WT with si-ctrl: 1.0 ± 0.03 , WT with si-UPF1: 0.91 ± 0.04). * Significantly different from those with si-ctrl treatment (Student's t-test, $P<0.05$). (F) The protein levels of UPF1 and wild-type and mutant pEGFP-PODXL detected by Western blot analysis after HEK 293T cells were sequentially transfected with si-UPF1 or si-ctrl and wild-type or mutant pEGFP-PODXL plasmids.

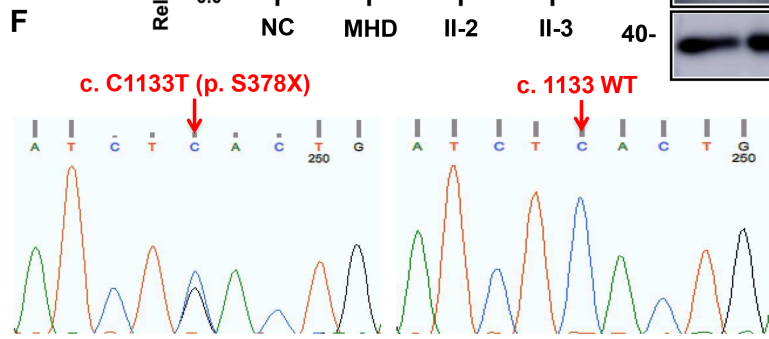
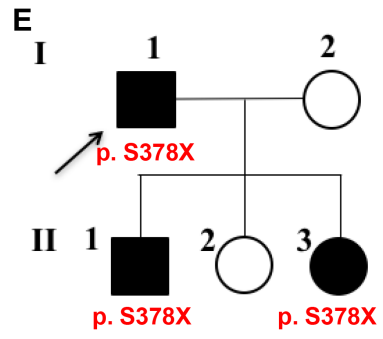
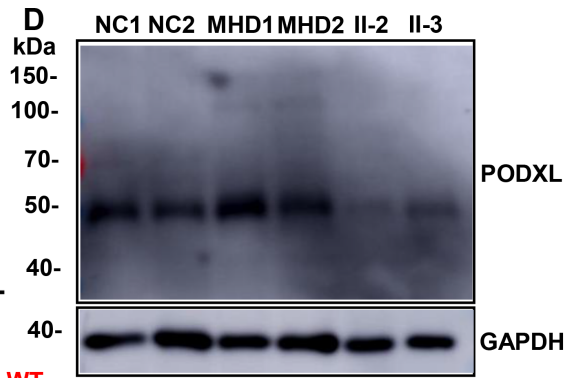
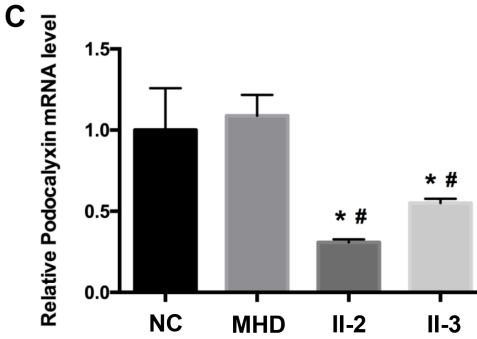
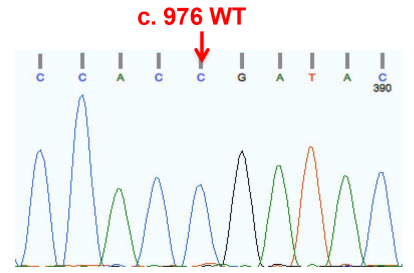
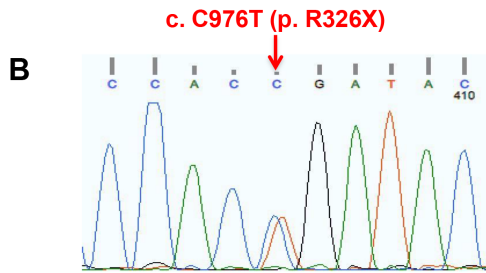
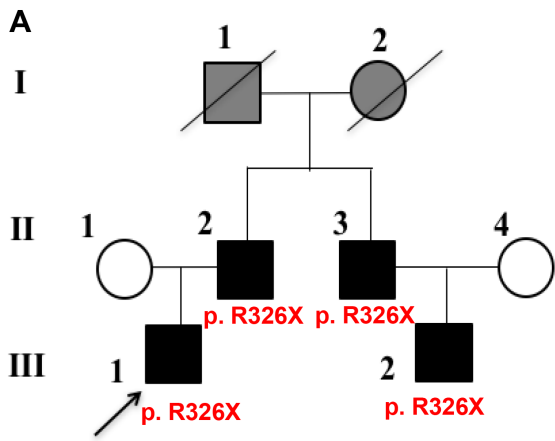
Figure 3: Effects of *PODXL* knockdown on activities of RhoA and ezrin in cultured podocyte. (A) *PODXL* siRNA transfection led to significant reduction of phosphorylated ezrin (p-ezrin) in the podocytes compared with controls. β -actin was included as a loading control. (B) Bar graph represented relative p-ezrin protein levels normalized against β -actin and data represented the mean \pm SD of 3 independent experiments (Mock: 1; NC-siRNA: 0.93 ± 0.04 ; *PODXL*-siRNA: 0.31 ± 0.03). *Significantly different from mock transfection group (ANOVA with post-test correction, $P<0.05$), #Significantly different from NC-siRNA transfection group

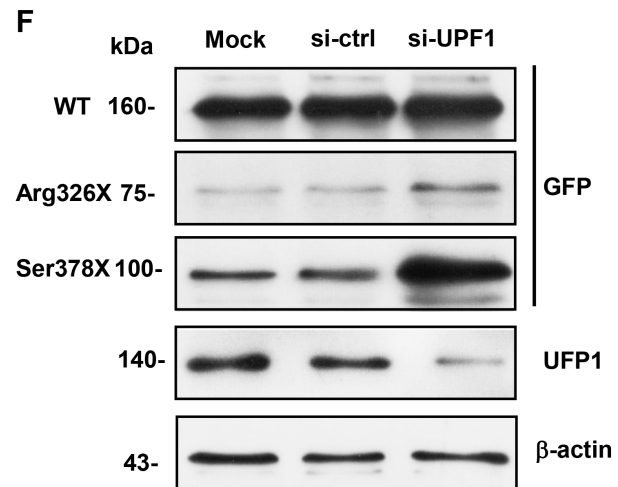
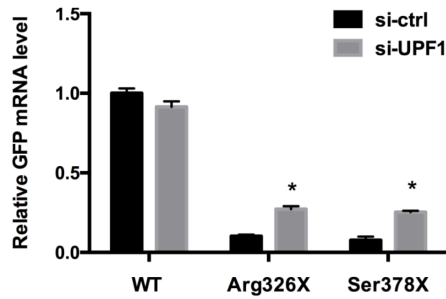
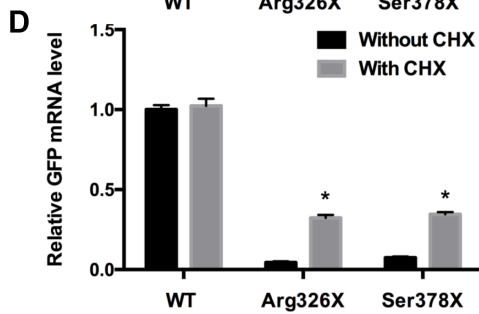
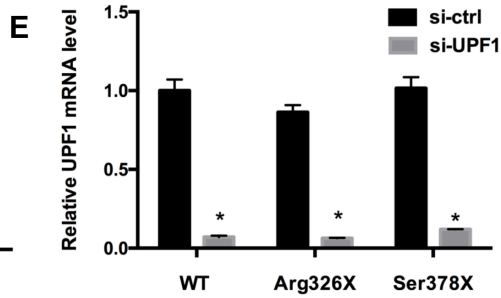
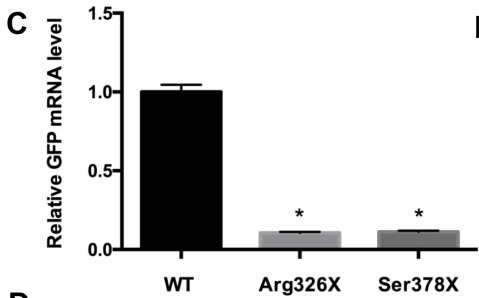
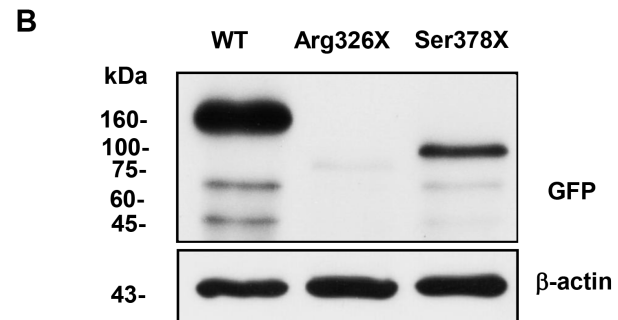
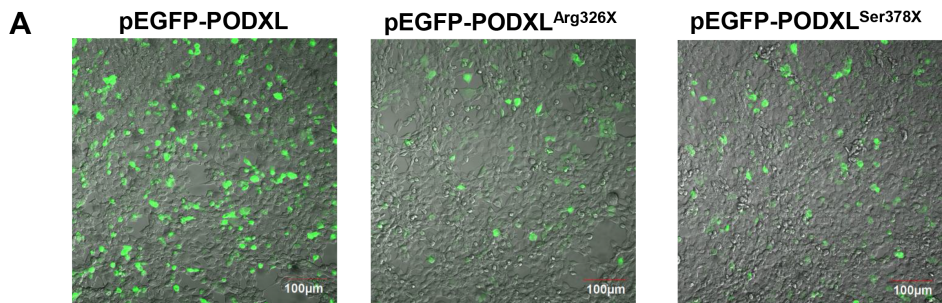
(ANOVA with post-test correction, $P<0.05$). (C) PODXL siRNA induced significant reduction of activated RhoA and the bar graph showed the relative RhoA G-LISA values in mock vector transfection group (0.43 ± 0.03), NC-siRNA transfection group (0.42 ± 0.03) and PODXL-siRNA group (0.16 ± 0.02). *Significantly different from mock transfection group (ANOVA with post-test correction, $P<0.05$), #Significantly different from NC-siRNA transfection group (ANOVA with post-test correction, $P<0.05$).

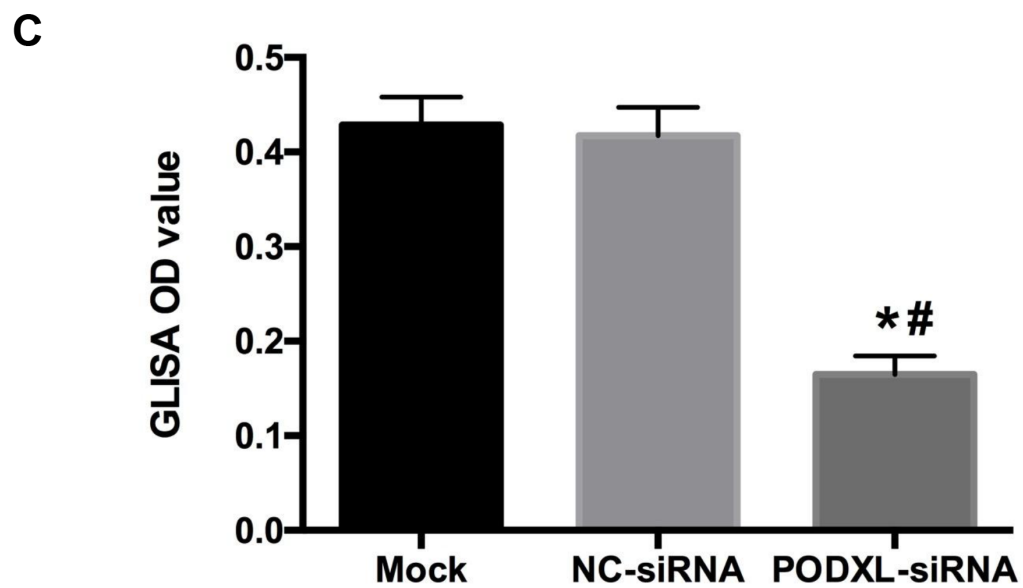
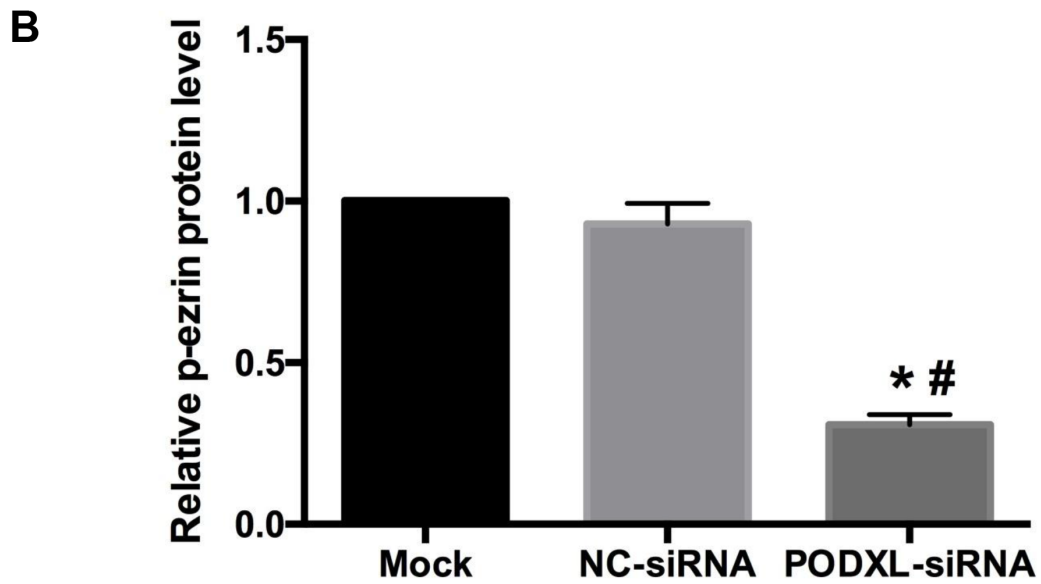
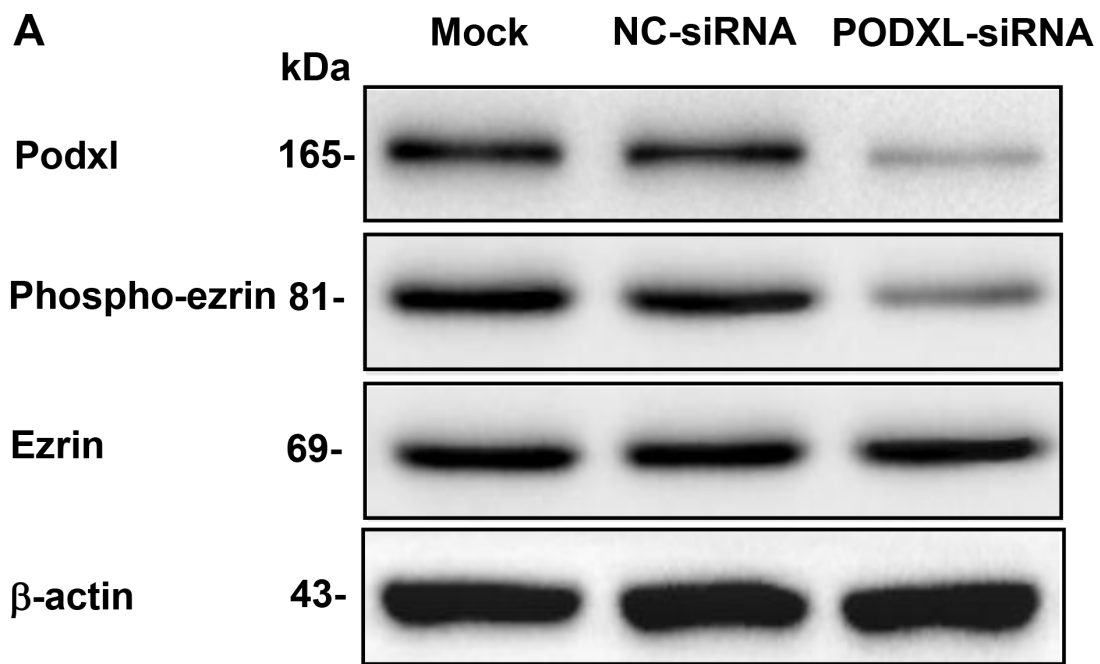
Figure 4: Effects of *PODXL* knockdown on podocyte mobility in cultured

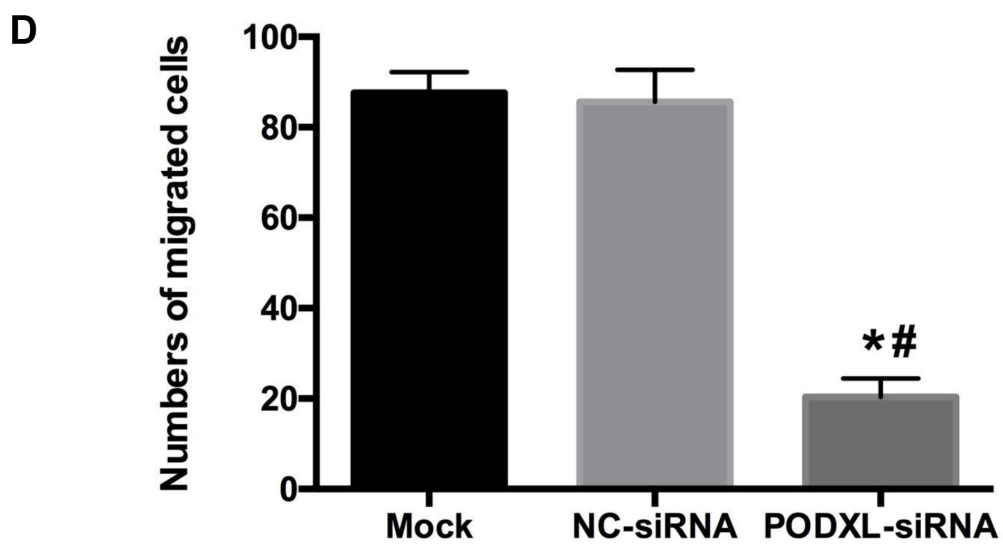
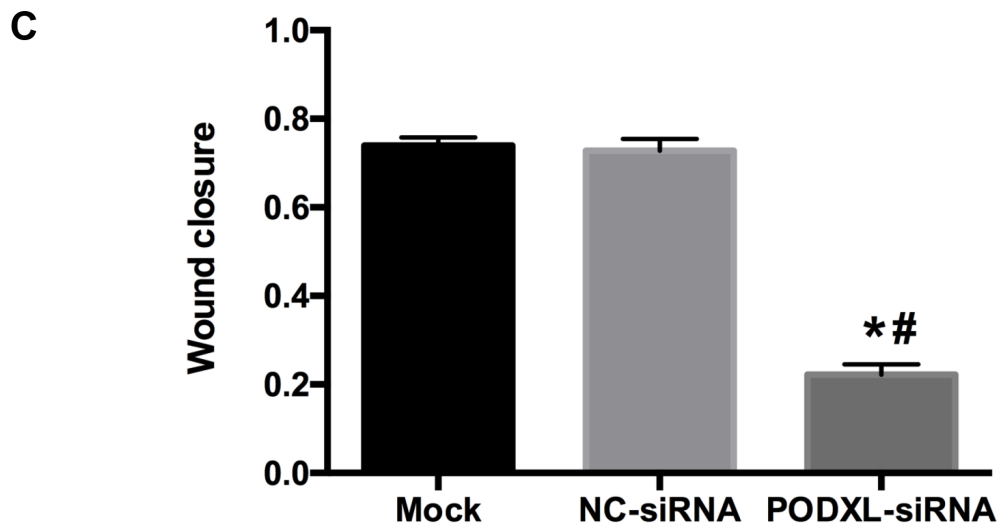
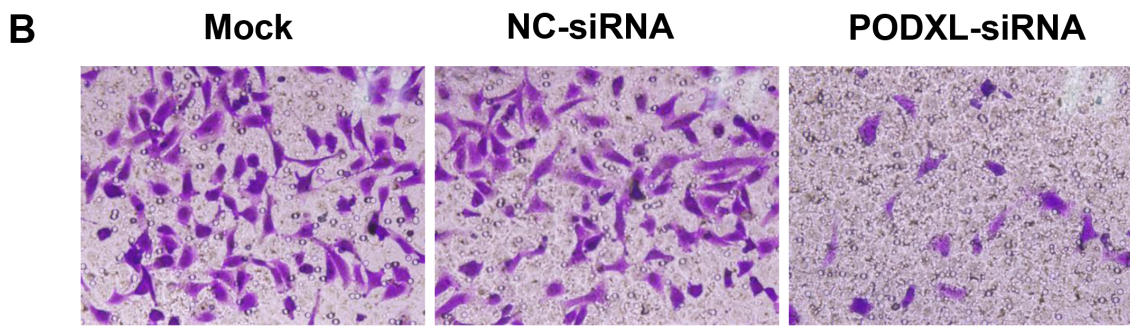
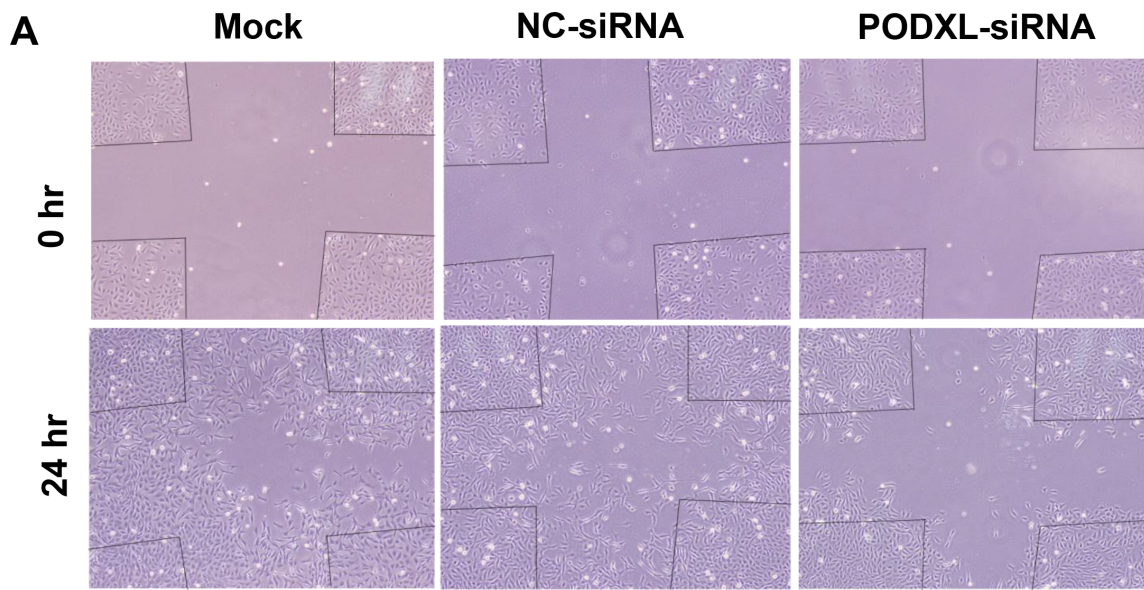
podocytes. The wound-healing assay (A) and the transwell migration assay (B) were performed. PODXL siRNA treatment significantly slowed podocyte migration after 24 hours compared with the podocytes in the control groups. Magnification: wound-healing assay $\times 10$; transwell migration assay $\times 40$. Bar graphs showed wound closure area in the scratches in the groups of cells that were treated differently after 24 hours (Mock: 0.74 ± 0.02 ; NC-siRNA: 0.73 ± 0.03 ; PODXL-siRNA: 0.22 ± 0.02) (C) and the numbers of migrating podocytes in the groups treated differently (Mock: 87.67 ± 4.51 ; NC-siRNA: 85.67 ± 7.02 ; PODXL-siRNA: 20.33 ± 4.16) (D). Data represent the mean \pm SD of 3 independent experiments. *Significantly different from mock transfection group (ANOVA with post-test correction, $P<0.05$), #Significantly different from NC-siRNA transfection group (ANOVA with post-test correction, $P<0.05$).

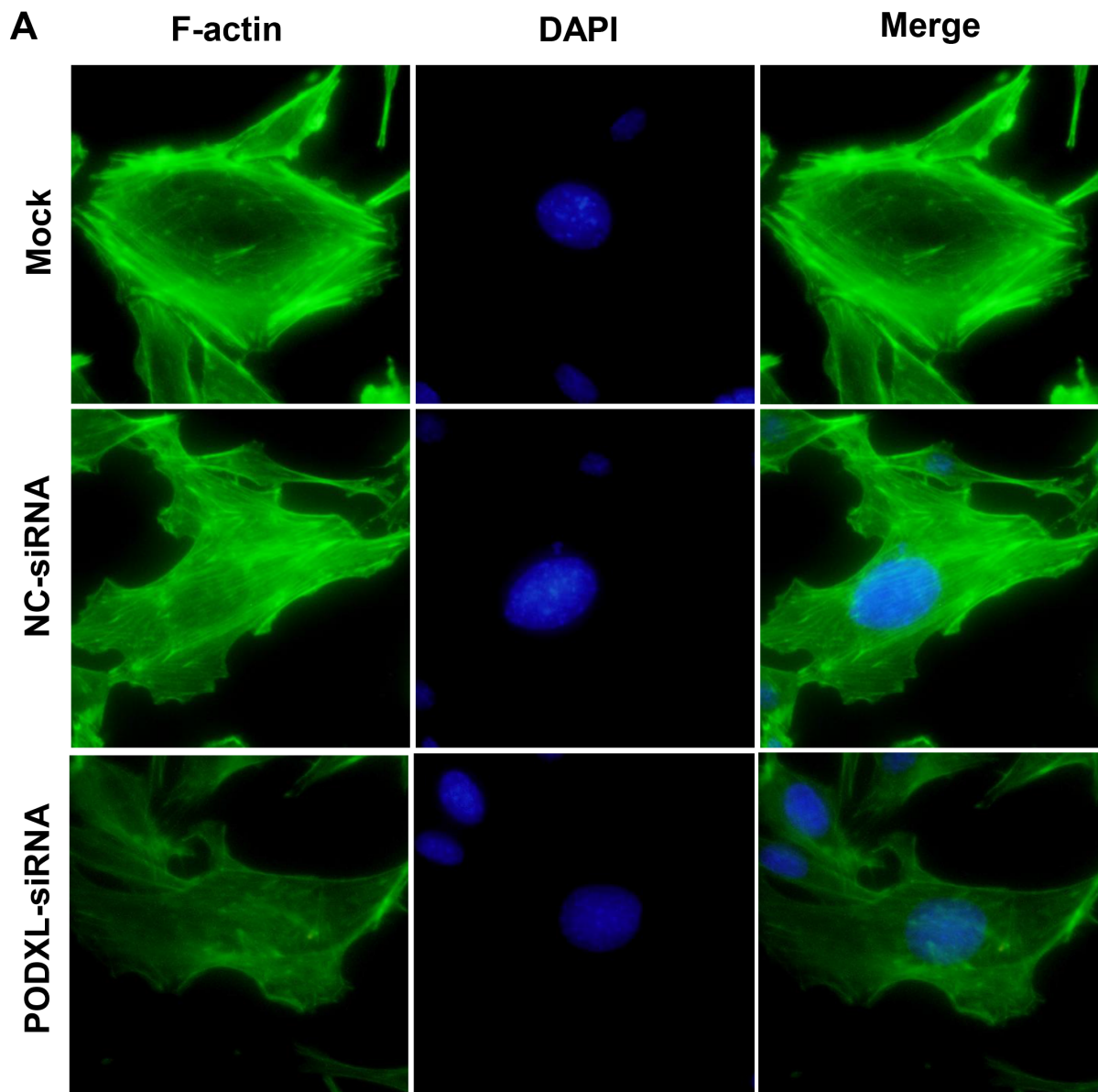
Figure 5: Effects of *PODXL* knockdown on F-actin stress fibers formation in cultured podocytes. (A) Representative results of phalloidin staining showing that *PODXL* siRNA induced significant reduction of F-actin fibers in cultured podocytes compared with controls. Magnification: 40×. (B) Quantification of the results in (A) (n=3) (Mock: 3117±246.8 ; NC-siRNA: 3027±293.3; *PODXL*-siRNA: 1371±140.8). *Significantly different from mock vector transfection group (ANOVA with post-test correction, $P<0.05$), #Significantly different from NC-siRNA transfection group (ANOVA with post-test correction, $P<0.05$).











B

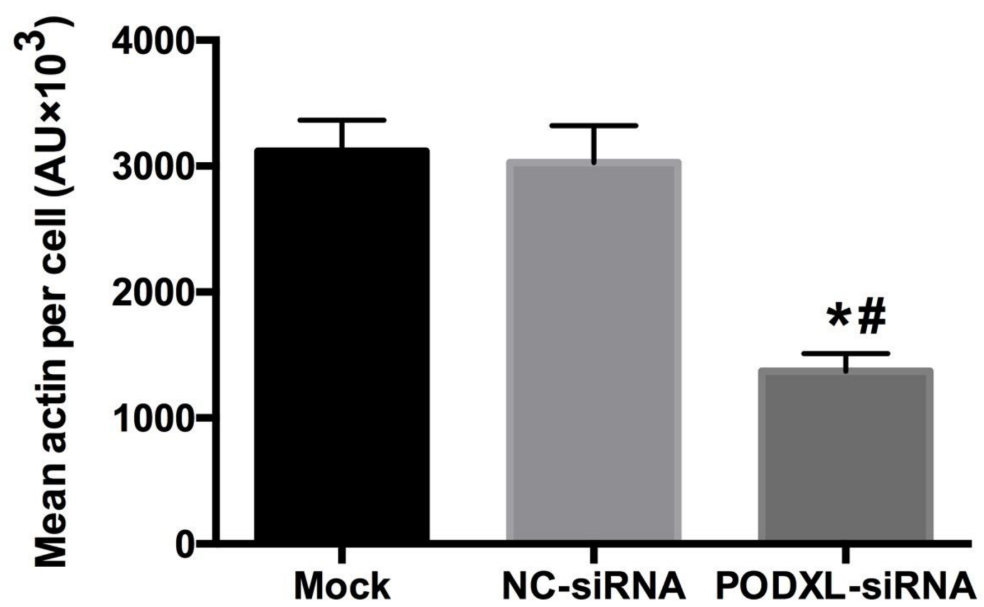


Table 1. Clinical characteristics of patients with *PODXL* non-sense mutations

Characteristics	Chinese Pedigree with p. Arg294X						Indian Pedigree p. Ser346X							
	II-2 (Male)		II-3 (Male)		III-1 (Male)		III-2 (Male)		I-1 (Male)		II-1 (Male)		II-3 (Female)	
	Onset	Last Follow-up	Onset	Last Follow-up	Onset	Last Follow-up	Onset	Last Follow-up	Onset	Last Follow-up	Onset	Last Follow-up	Onset	Last Follow-up
Age (y)	30	72	22	69	25	39	33	35	56	62	20	26	26	31
Urine ACR (mg/mmol)	30-100	50	<30	Anuria	100	150	30-50	50-100	313	351	308	118	101	80
Scr (μ mol/L)	NR	ESRD	NR	ESRD	NR	350	NR	NR	182	208	78	69	52	46
Haematuria (/HP)	2-3	3-5	5-8	Anuria	0-2	1-3	0	0	0	0	0	0	0	0
Hypertension	No	Yes	No	Yes	No	Yes	No	No	No	No	No	No	No	No
Renal biopsy findings	N/A	N/A	N/A	N/A	N/A	N/A	N/A	N/A	FSGS	N/A	FSGS	N/A	FSGS	N/A

Abbreviations: ACR, albumin: creatinine ratio (normal range <15 mg/mmol); ESRD, end-stage renal disease; FSGS, focal segmental glomerulosclerosis; N/A, not applicable; NR, within normal range; Scr, serum creatinine (normal range 35-97 μ mol/L).

Supplementary Methods

Flow cytometry

Approximately 1×10^6 PBMCs of different samples were washed twice with phosphate-buffered saline (PBS). After centrifugation, the cells were suspended in 100ul PBS containing CD45 antibody, eFluor450(eBioscience) and CD34 antibody, PE (Beckman Coulter). The samples were incubated for 30 minutes at room temperature (RT) in the dark. The samples were analyzed with the use of FACS cantoII (BD Biosciences) with Flowjo software (BD Biosciences).

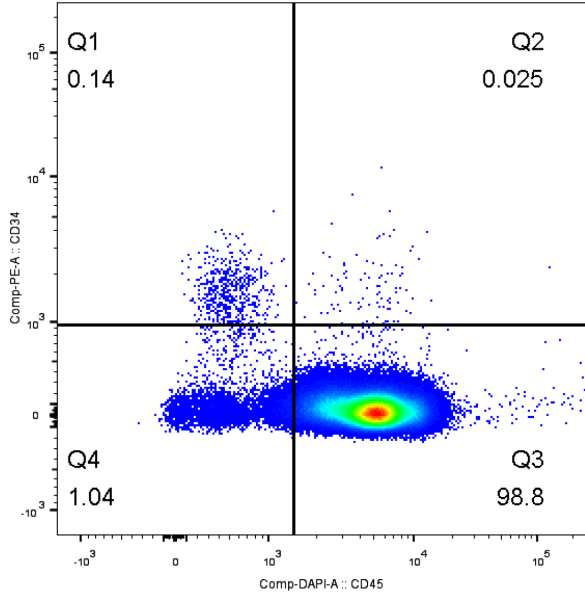
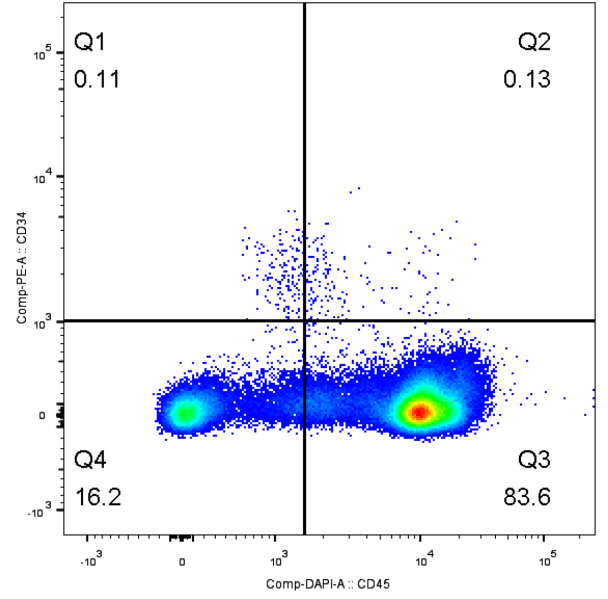
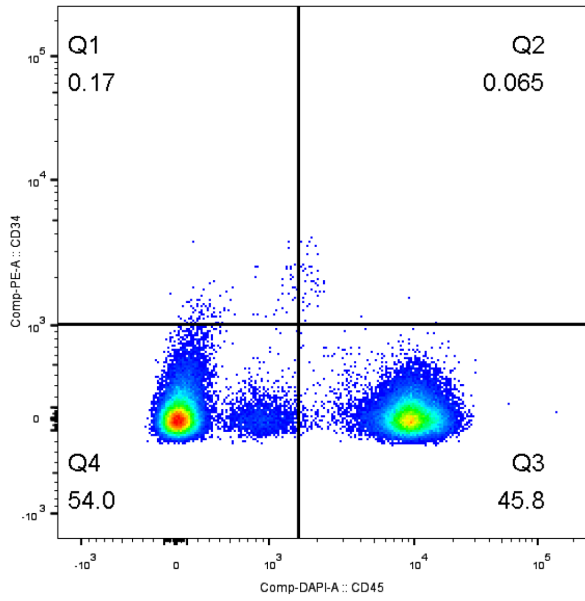
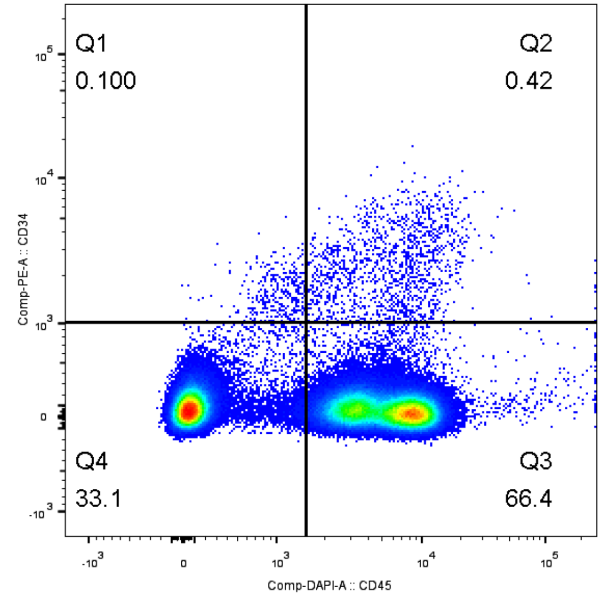
Detection of secreted podocalyxin from extracellular medium

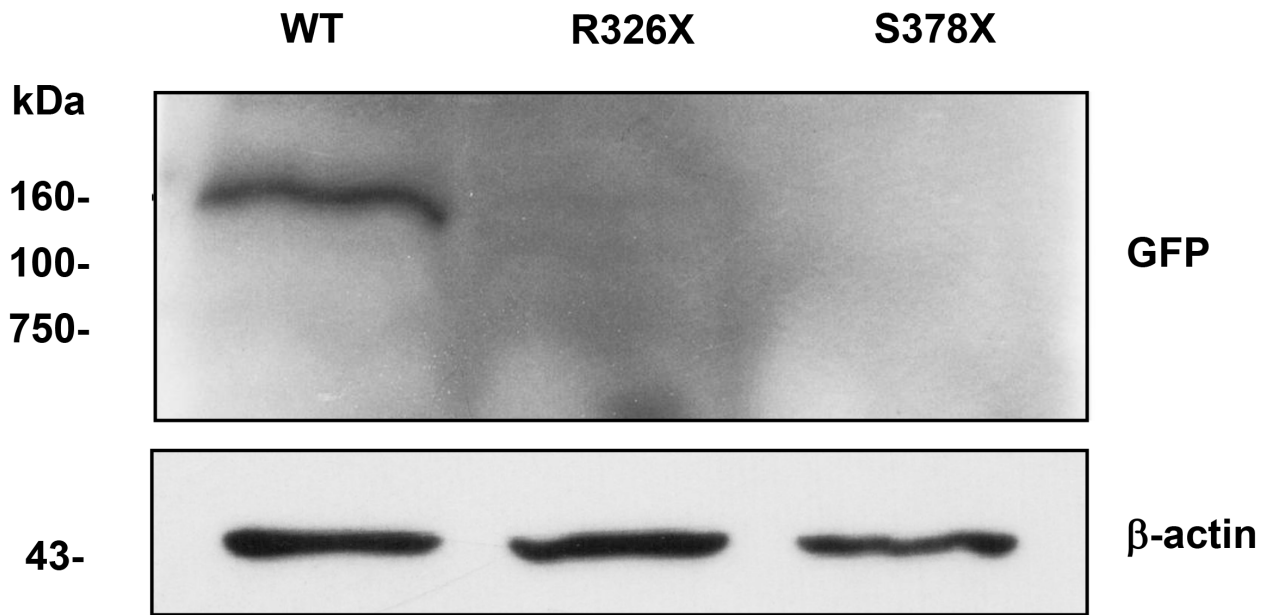
Transfected HEK 293T cells were cultured in 6-well plates with 10% FBS DMEM medium at 37°C and 5% CO₂. After 48hr, cells were washed with PBS three times then changed to serum-free DMEM medium for 8 hours. The culture medium (12ml) was collected and concentrated down to 500μL using Amicon Ultra 10K Centrifugal Filter (Merck Millipore). The concentrated culture medium were electrophoresed in SDS-PAGE and immunoblotted using the primary antibody against GFP antibody (Cell Signaling Technology) or β-actin (Cell Signaling Technology), followed by incubation with the appropriate secondary antibody. After immunoblotting, an ECL Plus Western Blotting System (GE Health) was used for detection.

Supplementary figure legends

Supplementary figure 1: Representative picture of CD34⁺CD45⁻ hematopoietic cells (% , upper left quadrant, Q1) from a healthy control (A), a maintenance hemodialysis patient control (B), II-2 (C) and II-3 (D) from the Chinese pedigree.

Supplementary figure 2: Soluble podocalyxin expression in concentrated culture medium of HEK 293T cells transfected with wild-type pEGFP-PODXL or mutant pEGFP-PODXL plasmids.

A**B****C****D**



Supplementary Table 1. Summary of whole exome sequencing data

	III-1 of the Chinese kindred	I-1 of the British-Indian kindred
Total_reads	85617212	87702844
Mapped_to_target_reads	60358467	61008084
Percentage	70.50	69.56
mapped_to_target_reads_plus_150bp	67836951	67865297
Percentage	79.23	77.38
Mean_coverage	112.33	115.04
Accessible Target_bases	33323618	33323618
Accessible Target_bases_1x	33020814	32942391
Percentage	99.09	98.86
Target_bases_5x	32733988	32576698
Percentage	98.23	97.76
Target_bases_10x	32429578	32230715
Percentage	97.32	96.72
Target_bases_20x	31578327	31306438
Percentage	94.76	93.95

Supplementary Table 2. Expression of CD34⁺CD45⁻ hematopoietic cells on peripheral blood mononuclear cells

Source of CD34 ⁺ CD45 ⁻ PBMC	% of Positive
Healthy controls (n=6)	0.15 ± 0.06
MHD patients with no <i>PODXL</i> nonsense mutations (n=6)	0.14 ± 0.04
II-2 of the Chinese pedigree	0.14 ± 0.04
II-3 of the Chinese pedigree	0.11 ± 0.02

The data represented the mean ± SD of 3 separate analyses.

Abbreviations: MHD, maintenance hemodialysis; PBMC, peripheral blood mononuclear cells.